Monsoon-induced zonal asymmetries in moisture transport cause anomalous Pacific precipitation minus evaporation

Geophysical Research Letters

RESEARCH LETTER
10.1029/2020GL088659

Key Points:
- Atlantic and Pacific $P-E$ (precipitation minus evaporation) asymmetry is primarily due to atmospheric moisture transport and precipitation
- Moisture fluxes into the polar ocean basins do not contribute notably to $P-E$ asymmetries between the Atlantic, Pacific, and Indian basins
- Deviations from zonal mean zonal moisture flux associated with the summer monsoon flow across Southeast Asia dominate the $P-E$ asymmetry

Supporting Information:
- Supporting Information S1

Correspondence to:
P. M. Craig,
philip.craig@reading.ac.uk

Citation:
Craig, P. M., Ferreira, D., & Methven, J. (2020). Monsoon-induced zonal asymmetries in moisture transport cause anomalous Pacific precipitation minus evaporation. *Geophysical Research Letters*, *47*, e2020GL088659. https://doi.org/10.1029/2020GL088659

Received 4 MAY 2020
Accepted 5 SEP 2020
Accepted article online 14 SEP 2020

Monsoon-Induced Zonal Asymmetries in Moisture Transport Cause Anomalous Pacific Precipitation Minus Evaporation

P. M. Craig[1], D. Ferreira[2], and J. Methven[2]

[1]National Centre for Atmospheric Science, Department of Meteorology, University of Reading, Reading, UK, [2]Department of Meteorology, University of Reading, Reading, UK

Abstract Basin-integrated precipitation minus evaporation ($P-E$) in the Pacific is near neutral while the Atlantic shows net evaporation. We link this $P-E$ asymmetry to atmospheric moisture fluxes across the boundaries of the ocean drainage basins. Adopting an objective approach based on a comparison between actual fluxes and a zonally averaged circulation, we show that the asymmetry is dominated by moisture fluxes associated with the monthly mean flow at low latitudes rather than by differences in moisture fluxes into the Southern Ocean and Arctic catchments. In boreal summer, the eastward moisture flux, due to the Asian Summer Monsoon flow, opposes the zonal mean westward flux in the Trade Winds and results in more positive $P-E$ over the Pacific than both the Atlantic and Indian Oceans, even in the annual mean. Our analysis reveals that moisture flux across Southeast Asia, rather than across Central America, is the dominant factor in the $P-E$ asymmetry.

1. Introduction

The contrast between Atlantic and Pacific sea surface salinity (SSS) is linked to the time-mean asymmetry in $P-E$ (precipitation minus evaporation) where the Atlantic $P-E \approx -0.5$ Sv ($1\,\text{Sv} \equiv 10^9\,\text{kg s}^{-1}$) and the Pacific is near neutral. Craig et al. (2017) have shown the consistency of these estimates obtained from a range of atmospheric and oceanic analysis techniques. Both the SSS and $P-E$ asymmetries have been linked to the existence of a meridional overturning circulation (MOC) in the Atlantic and absence of a Pacific MOC (Broecker, 1991; Ferreira et al., 2010) although there may also be a role for salt transport (see Ferreira et al., 2018, for a review).

Previous studies have suggested that enhanced northward heat transport in the Atlantic by the Atlantic MOC (Trenberth & Caron, 2001) results in stronger Atlantic evaporation and that the excess water vapor is transported in the Trade Winds across Central America to the Pacific causing weak net evaporation or net precipitation across the Pacific (Broecker, 1991). However, the Atlantic evaporation is only notably stronger in the subpolar region (Craig et al., 2017; Czaja, 2009; Emile-Geay et al., 2003; Warren, 1983; Wills & Schneider, 2015). There, sea surface temperatures are higher than in the Pacific (Manabe & Stouffer, 1988; Warren, 1983), and a greater fraction of the narrower basin is affected by advection of air off continents with low relative humidity (Schmitt et al., 1989) resulting in stronger area-averaged evaporation. However, the $P-E$ asymmetry exists at all latitudes (Craig et al., 2017). South of 30°N, the $P-E$ asymmetry is dominated by greater precipitation per unit area over the Pacific than the Atlantic. At the basin scale, evaporation rates per unit area across the Atlantic, Pacific, and Indian Oceans are similar (Craig et al., 2017), and therefore, precipitation differences dominate the $P-E$ asymmetry.

The vertical integral of the atmospheric moisture budget implies that, in a sufficiently long time average, the asymmetry in $P-E$ can only be balanced by differences in the convergence of atmospheric moisture flux into each ocean catchment. The drainage basins of the Atlantic, Pacific, and Indian Oceans are defined by their continental divides, where they exist, and connected by segments across sea where necessary (see Figure 1 and further details below).

The hypothesis that strong atmospheric moisture transport by the Trade Winds across Central America (Figure 2) is the cause of the $P-E$ asymmetry between the Atlantic and Pacific appears often in the literature. Some authors specifically refer to the Isthmus of Panama (a very narrow strip of land) as the location of

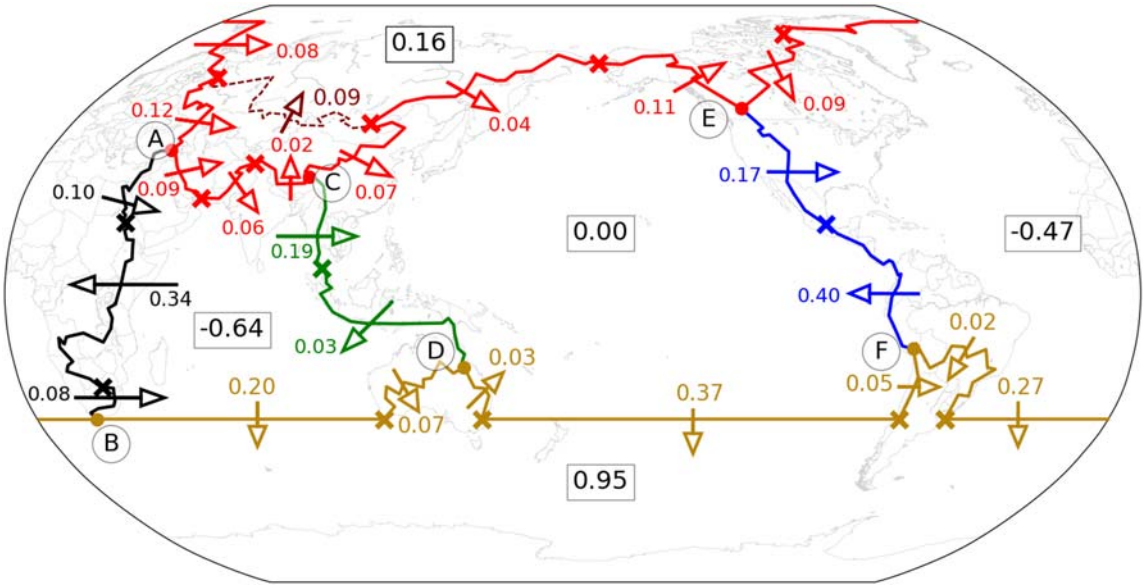

Figure 1. Vertically and horizontally integrated annual mean (1979–2014) ERA-Interim moisture fluxes normal to each catchment boundary (Q_{XY}) and basin-integrated precipitation minus evaporation ($\overline{P-E}$, boxes) calculated from Q_{XY} using Equation 1. The large dots (labeled A, B, C, D, E, and F) indicate the nodes of each sector of the Arctic (red) and Southern Ocean (gold) catchment boundaries where they meet the American (blue), African (black), and Southeast Asian (green) catchment boundaries. The crosses show where the catchment boundaries are split into segments either based on the change in net direction of Q_{XY} or for geographical reasons. All units are Sverdrups ($1\,\mathrm{Sv} \equiv 10^9\,\mathrm{kg\,s^{-1}}$).

the Atlantic-to-Pacific moisture transport (Leduc et al., 2007; Lohmann, 2003; Sinha et al., 2012; Zaucker & Broecker, 1992), and other authors refer to Central America in general (Broecker, 1991; Richter & Xie, 2010; Schmittner et al., 2011; Wang et al., 2013). The emphasis on the moisture transport over Central America in explaining the $P-E$ asymmetry is based on two elements: (1) This flux is one of the strongest and is larger than the moisture flux over Africa at similar latitudes, and (2) it is the shortest pathway from the Atlantic to the Pacific drainage basins.

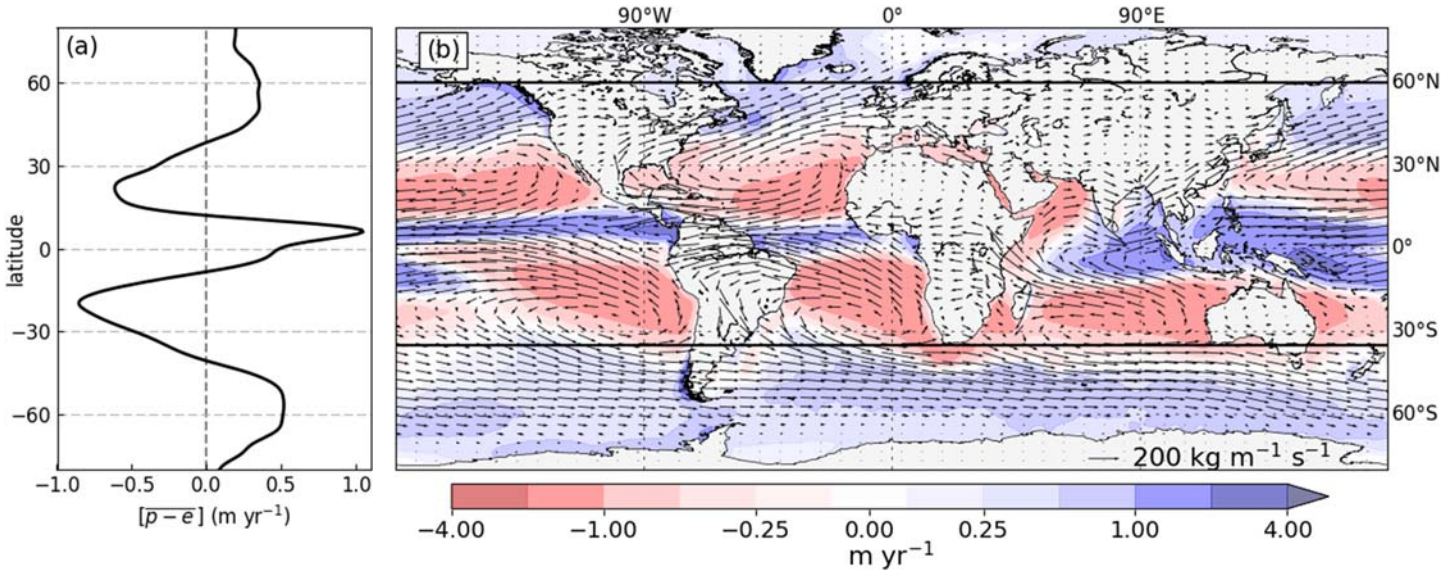

Figure 2. Annual mean (1979–2014) ERA-Interim $p-e$ (lowercase p and e represent local precipitation and evaporation rates) from vertically integrated moisture flux divergence: (a) zonal mean $[\overline{p-e}]$ from 80°S to 80°N and (b) global $\overline{p-e}$ (overbar denotes time mean) across the oceans (contours) and vertically integrated moisture fluxes (arrows—see bottom right for scale). The black lines along 60°N and 35°S highlight the ocean basin latitude range referred to in the text.

Point (2) assumes that all Atlantic-to-Pacific atmospheric moisture transport across Central America is evaporated from the subtropical Atlantic and precipitated across the tropical Pacific (Leduc et al., 2007; Richter & Xie, 2010). This Eulerian understanding of the hydrological cycle ignores long-range atmospheric transport and potential remote sources of moisture and will be addressed in a separate paper.

Focusing on (1), there is indeed a strong moisture transport across Central America (0.29–0.72 Sv; Richter & Xie, 2010) as the lower orography relative to North and South America results in a reduced rain shadow effect while the moisture transport over Africa at similar latitudes is comparatively smaller (Broecker, 1991; Figure 2b). However, it could be argued equally that the weakness of the moisture flux over Africa explains the divergent moisture transport over the Atlantic drainage basin. In other words, previous studies (cited above) highlighted the atmospheric moisture transport across Central America without providing a clear benchmark to objectively compare the relative contributions of the fluxes around the drainage basin to the asymmetry.

Here, to study the Atlantic-Pacific $P-E$ asymmetry, we suggest that the zonally averaged atmospheric state is a useful reference state to compare moisture fluxes, especially those across the meridionally orientated boundaries (AB, CD, and EF in Figure 1). One salient point is that the normal moisture fluxes, integrated along these meridionally orientated boundaries, could not contribute to the $P-E$ asymmetries between basins if they were all equal to the zonal average zonal moisture flux. It is only deviations from the zonal average flux across these boundaries, or the fluxes into the Southern Ocean (SO) or Arctic basins, that could contribute to the $P-E$ asymmetries. Critically, the normal moisture flux across the American catchment boundary is approximately equal to the integral of the zonal mean zonal moisture flux across the same latitude range (Ferreira et al., 2018). It is therefore unlikely that the flux across the American catchment boundary contributes to the $P-E$ asymmetry between the Atlantic and Pacific as was suggested by previous studies.

Another salient feature arises from consideration of the zonally averaged $P-E$. Figure 2a shows that the time-mean zonal mean $P-E$ is negative in the subtropics and positive in the equatorial region and at high latitudes (integrating to zero globally). Therefore, integrated over the latitude range of the Pacific Ocean basin, from approximately 35°S to 60°N, the zonal mean $P-E$ must be negative, as this range excludes the zone of net precipitation in the southern hemisphere high latitudes (Figure 2b). $P-E$ for the Pacific and Atlantic Ocean basins can be considered anomalous to the extent that it deviates from the negative value obtained by integrating the zonal mean distribution over the area of the basin. The negative $P-E$ over the Atlantic is less anomalous than the neutral $P-E$ of the Pacific.

In this paper, we will address the time-mean $P-E$ asymmetry. To this end, we evaluate, in a quantitative and objective manner, the contributions of the moisture fluxes across catchment boundaries to the asymmetry using the zonally averaged state as a reference point. Our analysis notably reveals that the moisture flux across Southeast Asia is the dominant factor in the $P-E$ asymmetry.

2. Data and Methods

Throughout this paper we use vertically integrated horizontal water vapor fluxes from ERA-Interim reanalysis (Dee et al., 2011) over the period 1979 to 2014. The vertical integral of moisture flux normal to catchment boundaries surrounding the ocean drainage basins (defined in the data set, Craig, 2019) is calculated at points along the boundaries using the formula:

$$Q_n = \frac{1}{g}\int_0^1 \overline{q\mathbf{v}}\cdot\hat{\mathbf{n}}\frac{\partial p}{\partial \eta}\,d\eta, \tag{1}$$

where $\hat{\mathbf{n}}$ is the unit vector normal to the boundary, $\mathbf{v}$ is the horizontal wind vector, q is specific humidity, η is the vertical coordinate of the ERA-Interim data, p is pressure, and the overbar denotes a time mean. The contributions to Q_n from the monthly mean flow (Q_n^m) and from submonthly moisture fluxes (Qn') are calculated using Reynolds averaging:

$$\overline{q\mathbf{v}}\cdot\hat{\mathbf{n}} = \bar{q}\,\overline{\mathbf{v}}\cdot\hat{\mathbf{n}} + \overline{q'\mathbf{v}'}\cdot\hat{\mathbf{n}}. \tag{2}$$

The integral of Q_n along a catchment boundary between any two points X and Y (see Figure 1) is expressed as Q_{XY}. These are linked precisely to $P-E$ through the divergence theorem (see supporting information [SI]).

Note that Craig et al. (2017) present $E-P-R$ including the runoff, R, estimated with Dai and Trenberth's (2002) river discharge data set. Here, $\overline{P-E}$ for an ocean drainage basin incorporates R as it is approximately equal to net precipitation over land assuming that storage fluxes are relatively small in the monthly average. See the SI for more details on the data and methods.

3. Annual Mean Moisture Fluxes and Basin-Integrated $P-E$

The annual average $P-E$ for the five ocean basins and the integral fluxes across the various segments of the boundaries surrounding the basin catchments are shown in Figure 1. General features are that moisture fluxes are mainly crossing the boundaries eastward in the extratropics, and also poleward across 35°S into the SO basin. At low latitudes, moisture crosses the boundaries westward in the Trade Winds, with the notable exception of Southeast Asia (boundary CD) where the annual average flux is in the opposite direction.

Across the American boundary (EF) westward atmospheric moisture transport at low latitudes is partially offset by eastward transport in the midlatitudes. In contrast, across the northern section of the Southeast Asian catchment boundary, there is an eastward moisture flux associated with the annual mean flow across India and the Bay of Bengal. The $\overline{P-E}$ values calculated from Q_{XY} surrounding the Atlantic, Indian, and Pacific Oceans are consistent with the various estimates compared in Craig et al. (2017). Other authors have presented maps similar to Figure 1 (Levang & Schmitt, 2015; Rodriguez et al., 2011; Singh et al., 2016), but in some estimates Q_{CD} is weaker than, or of opposing sign to, Figure 1. This appears to be a consequence of coarse resolution and problems with representing the Walker Circulation (Schiemann et al., 2014) and wind over the equatorial Indian Ocean (Goswami & Sengupta, 2003). Some studies present a CD boundary differing substantially from Figure 2 which results in a weaker Q_{CD} but does not substantially change the $\overline{P-E}$ asymmetries. These estimates are discussed in more detail in the SI. Despite these specific differences, basin scale $\overline{P-E}$ from ERA-Interim are in good agreement with estimates based on both atmospheric and oceanographic data using various different methodologies (Craig et al., 2017). The area-averaged residual between $\overline{P-E}$ calculated from moisture flux divergence and from the separate precipitation and evaporation fluxes is also small for each ocean basin.

A common interpretation of Figure 1 is that the westward Atlantic-to-Pacific transport across the southern end of the American boundary (0.40 Sv) dominates the $\overline{P-E}$ asymmetry as it is the largest flux entering the Pacific (Broecker, 1991; Richter & Xie, 2010; Zaucker & Broecker, 1992). However, this ignores the net eastward Indian-to-Pacific transport, Q_{CD}, across Southeast Asia (0.16 Sv). Atmospheric moisture converges into the Pacific drainage basin across both its western (CD) and eastern (EF) boundaries while the net transport is westward across both the western (EF) and eastern (AB) boundaries of the Atlantic basin. There is also net export of atmospheric moisture across all four catchment boundaries of the Indian drainage basin (resulting in strong net moisture flux divergence), and therefore, the Indian Ocean acts as a source of moisture for both the Atlantic and Pacific Oceans (Craig, 2018; Stohl & James, 2005).

Submonthly moisture fluxes across the Arctic and SO boundaries are always poleward (with the exception of the River Plate drainage basin—see Figure S1) reflecting the net poleward moisture transport in midlatitude weather systems (Dey & Döös, 2019; Pfahl et al., 2015). Submonthly poleward fluxes across 35°S to the SO are similar per unit length along each sector (Table S2) and therefore cannot account for the Atlantic/Pacific $\overline{P-E}$ asymmetry. Similar conclusions can be drawn for the submonthly fluxes into the Arctic; fluxes associated with the monthly mean flow into the polar basins are discussed in sections 5.1 and 5.2.

The submonthly fluxes across the boundaries between the Atlantic, Pacific, and Indian Oceans are very small compared to those associated with the monthly mean flow (Figure S1). The $\overline{P-E}$ asymmetry is therefore dominated by the monthly mean flow across the African, Southeast Asian, and American boundaries.

4. Seasonal Cycle in Moisture Fluxes and $P-E$

The Atlantic/Pacific $\overline{P-E}$ asymmetry is greatest in JJA (>1 Sv) when the net Southeast Asian flux Q_{CD} is eastward (0.59 Sv), associated with the Asian Summer Monsoon, and the westward net flux across the Americas, Q_{EF}, peaks (0.38 Sv) associated with the maximum strength of the Caribbean low-level jet (LLJ) (Wang et al., 2013). Both converge moisture into the Pacific basin, resulting in $\overline{P-E}=0.55$ Sv in JJA (Figure 3c). The JJA peak in Q_{EF} coincides with minimum African flux, Q_{AB} (0.08 Sv), as the Somali LLJ diverts moisture away from Africa (Riddle & Cook, 2008) thus contributing to peak Atlantic net evaporation (−0.63 Sv, Figure 3c). The moisture storage term, $\partial(TCWV)/\partial t$ (Equation 1 in SI), is more important in the seasonal

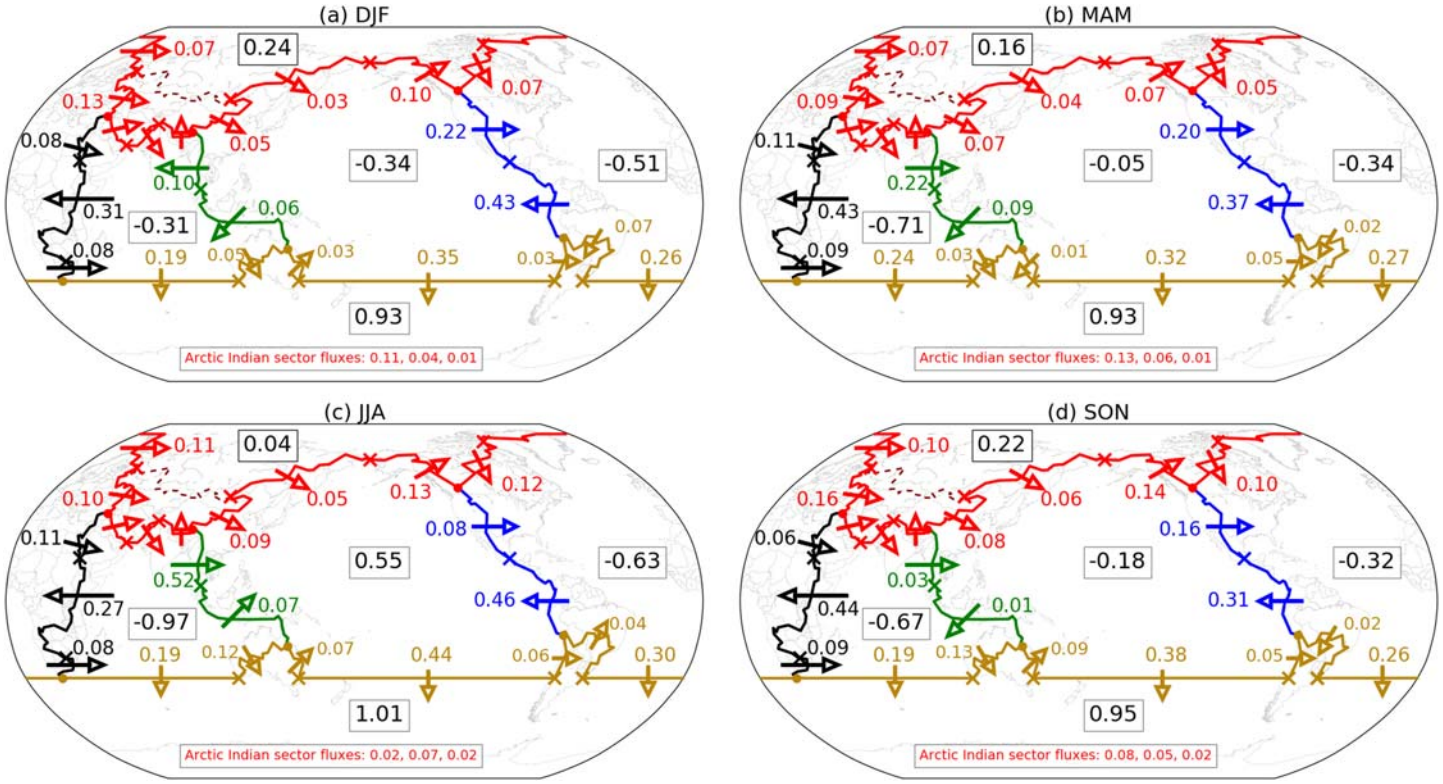

Figure 3. Climatological seasonal means (1979–2014) of $\overline{P-E}$ (boxes) and vertically and horizontally integrated moisture fluxes normal to each catchment boundary (arrows) split into sections based on geographic locations or change in the net direction of annual mean Q_n. All values are in Sverdrups ($1\,\mathrm{Sv} \equiv 10^9\,\mathrm{kg\,s^{-1}}$) and rounded to two significant figures.

cycle than in annual climatologies (Berrisford et al., 2011; Trenberth et al., 2011) but is only significant in the Pacific in JJA where it exceeds the divergence of Q_n by 0.01 Sv (Table S1).

The seasonal cycle of the Atlantic/Pacific $\overline{P-E}$ asymmetry is therefore strongly influenced by the meteorology of the Indian Ocean and the dynamics of the Asian Monsoon (Baker et al., 2015; Stohl & James, 2005; Volonté et al., 2019) as the only flux to change direction with season is Q_{CD}. The annual mean moisture flux field (Figure 2b) over the Indian Ocean, Maritime Continent, and North-West Pacific is dominated by JJA, as is Pacific $\overline{P-E}$ since it is negative during the rest of the year, but strongly positive in JJA, enabling the Pacific basin to be neutral in the annual mean (Figure 3). Emile-Geay et al. (2003) first suggested a role for the Asian Monsoon in the $\overline{P-E}$ asymmetry but only for the subpolar regions, while Craig et al. (2017) showed that the $\overline{P-E}$ asymmetry is dominated by stronger precipitation per unit area south of 30°N across the Pacific.

5. Understanding the $P-E$ Asymmetry by a Process of Elimination

The evidence has now been presented which will enable the deduction that the atmospheric moisture flux across Southeast Asia (the catchment boundary CD) is the dominant reason for the asymmetry in $P-E$ integrated over the Pacific compared with the Atlantic and Indian Ocean basins. The argument detailed below follows a process of elimination where the influence of moisture exchange with the Arctic and SO catchments are discounted and so are submonthly moisture fluxes at low latitudes. The final argument regards the moisture flux associated with the monthly mean flow across the three boundaries AB, CD, and EF.

5.1. Poleward Flux Across 35°S Into the SO Catchment

The net moisture flux poleward across 35°S is strongest in the Pacific sector (0.37 Sv) and weakest in the Indian sector (0.20 Sv) (Figure 1). However, the relative widths of the basins at 35°S (the Pacific is wider than the Atlantic and Indian Oceans by a factor of 1.8 and 1.5, respectively) dominate this variation. Submonthly fluxes are approximately equal when scaled by unit length along the boundary and therefore do not make a significant contribution to asymmetries in $\overline{P-E}$ (Table S2).

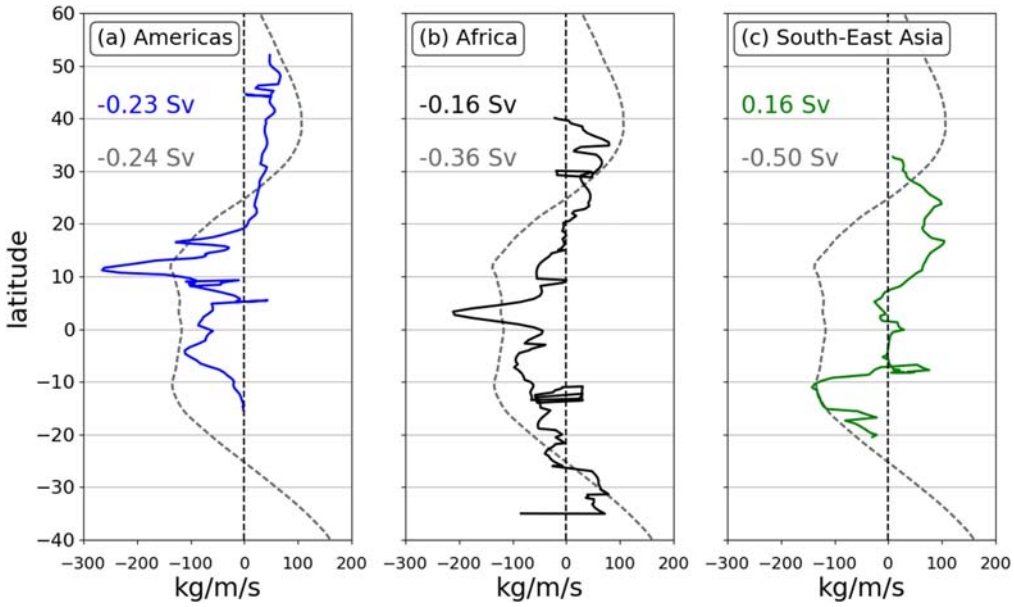

Figure 4. Comparison between the zonal mean zonal moisture flux ($[\overline{qu}]$, dashed lines) and the profile of the moisture flux normal to the (a) American, (b) African, and (c) Southeast Asian catchment boundaries (Q_n, solid lines). The colored numbers show the integrated fluxes, Q_{EF}, Q_{AB}, and Q_{CD}, for the respective catchment boundaries, and the gray numbers show the integral of $[\overline{qu}]$ between the latitude limits of each catchment boundary.

However, an asymmetry is found in Q_n^m: Q_n^m is an order of magnitude larger in the Atlantic than in the Pacific (possible reasons for this are discussed in the SI). Nevertheless, this Q_n^m asymmetry is small compared with the difference in $\overline{P-E}$ between the Pacific and Atlantic.

5.2. Moisture Exchange With Arctic

Atmospheric moisture imported into the Pacific drainage basin across Asia between the Himalayas and Bering Strait (0.11 Sv, Figure 1) is balanced by moisture exported across Canada and Alaska in the mid-latitude westerlies. Therefore, net Q_{CE} across the Pacific sector of the Arctic catchment boundary is approximately zero. Moisture imported across Canada into the Atlantic basin (0.09 Sv) is almost balanced by atmospheric moisture export into the Arctic (0.08 Sv) at the end of the North Atlantic storm track. However, net normal moisture flux across the Atlantic sector of the Arctic catchment boundary is dominated by zonal transport of 0.12 Sv across Europe into the Central Asian endorheic basin (i.e., isolated from the global ocean, but here counted as part of the Arctic basin) where $\overline{P-E} \approx 0$ Sv (Stohl & James, 2005). This results in a net export of atmospheric moisture from the Atlantic basin into the Arctic basin which contributes 0.11 Sv to the net negative $\overline{P-E}$ of the Atlantic.

This asymmetry is related to the shape of the Arctic catchment boundary (Figure 1). The Atlantic sector extends further south at its eastern end (Turkey) than the Pacific sector (southern Canada), so zonal moisture fluxes act to export moisture from the Atlantic into the Arctic across Eastern Europe. This accounts for the majority of the net positive $\overline{P-E}$ of the Arctic basin. The remainder of moisture flux convergence into the Arctic basin comes across the neighboring boundary over the Middle East from the Indian Ocean basin.

As introduced in section 3, the submonthly flux Q_n' across boundaries AC, CE, and EA is directed everywhere into the Arctic and does not contribute significantly to the $P-E$ asymmetry. However, transport by the monthly mean flow, Q_n^m, from the Atlantic into the Arctic does contribute 0.11 Sv to the asymmetry (making $P-E$ more negative for the Atlantic) since the net flux from the Pacific into the Arctic is approximately zero.

5.3. Anomalous Moisture Flux Across the Meridional Boundaries

As discussed in section 1, the moisture fluxes across the "meridional boundaries" AB, CD, and EF (Figure 1) can only contribute substantially to the $\overline{P-E}$ asymmetry if they differ, when integrated, from the zonal mean flux across the same latitude limits—otherwise just as much moisture would leave as entered each catchment across these boundaries. Figure 4 compares profiles of American, African, and Southeast Asian Q_n to the vertical integral of the zonal mean zonal moisture flux, $[\overline{qu}]$.

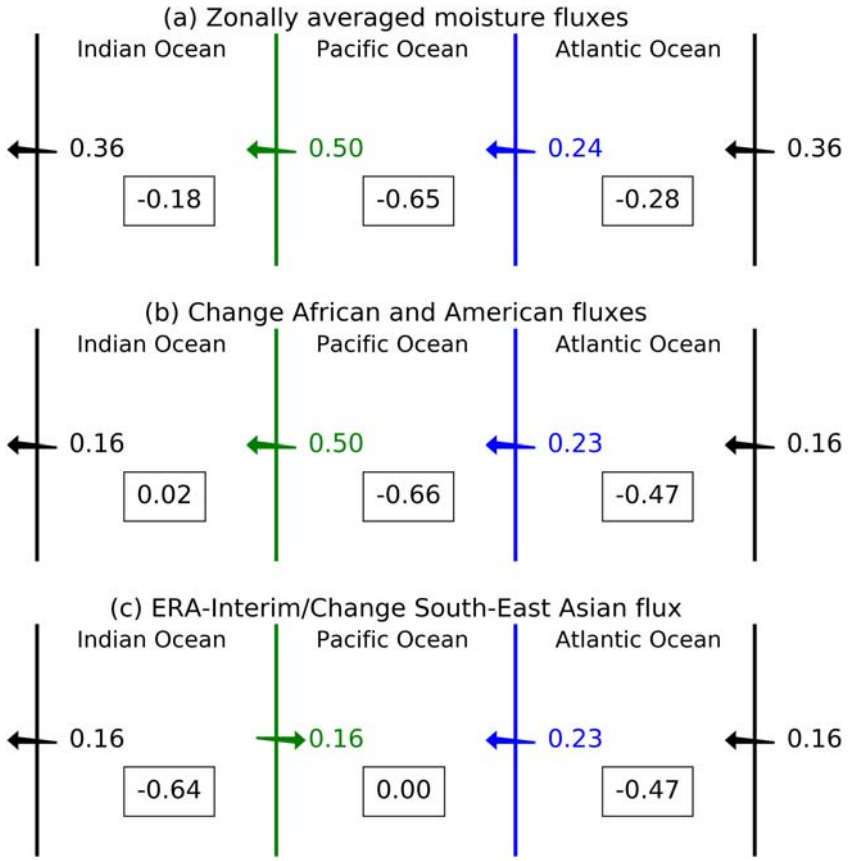

Figure 5. A thought experiment illustrating the influence of integral moisture fluxes across the catchment boundaries between the Atlantic, Indian, and Pacific Oceans. (a) Basin-integrated $\overline{P-E}$ (values in boxes) in the hypothetical situation that the normal fluxes across boundaries AB, CD, and EF were equal to zonal mean zonal moisture fluxes (gray numbers from Figure 4). (b) Reverting the fluxes across the African and American catchment boundaries to the observed values Q_{AB} and Q_{EF} and consequences for $\overline{P-E}$. (c) Reverting the flux across the Southeast Asian boundary to the observed value, Q_{CD}, recovering the ERA-Interim "real-world" estimates in all catchments. Note that moisture transports across the Arctic and Antarctic catchments remain unchanged and the latitude ranges for the American, African, and Southeast Asian catchment boundaries are exactly the same as those used in Figure 1. Fluxes and $\overline{P-E}$ are given in Sv.

The integral flux across the American boundary, Q_{EF}, almost matches the integral of $[\overline{qu}]$ across the same range of latitudes with a difference of only 0.01 Sv (Figure 4a). The most significant deviation of Q_n from $[\overline{qu}]$ occurs at 11°N above Lake Nicaragua in the Papagayo jet (Clarke, 1988) with a peak at 265 kg m^{-1} s^{-1}. The other peaks along Central America are at 17°N through the Chivela Pass from the Tehuantepec jet and at 9°N from the Panama jet (Steenburgh et al., 1998). Above Panama, Q_{EF} is less than $[\overline{qu}]$, so, contrary to previous literature (Leduc et al., 2007; Lohmann, 2003; Sinha et al., 2012; Zaucker & Broecker, 1992), moisture flux across Panama cannot be the dominant aspect of the $\overline{P-E}$ asymmetry.

The profile of African Q_n also bears some similarity to $[\overline{qu}]$ with a peak at 3°N (210 kg m^{-1} s^{-1}) in northern Kenya from the Turkana LLJ between the Ethiopian Highlands and East African Highlands (Nicholson, 2016). The integral flux Q_{AB} has the same sign as the integral of $[\overline{qu}]$ between the corresponding latitudes but is 0.20 Sv weaker (Figure 4b).

The profile of Southeast Asian flux, Q_{EF}, paints a very different picture to its American and African counterparts (Figure 4c). Deviations from $[\overline{qu}]$ along the Southeast Asian catchment boundary are far larger than those along the American and African catchment boundaries. Much of Q_n is of opposite sign to $[\overline{qu}]$, particularly across Thailand. The two only match between 10°S and 15°S above the Torres Strait between Australia and Papua New Guinea. The integral Q_{CD} is therefore of opposite sign to the corresponding integral of $[\overline{qu}]$, giving a net anomalous moisture export of 0.66 Sv from the Indian Ocean drainage basin to the Pacific.

To demonstrate the role of deviations of the integral moisture fluxes Q_{AB}, Q_{CD}, and Q_{EF} from $[\overline{qu}]$ in setting the $\overline{P-E}$ asymmetry, we conduct a thought experiment by considering a zonally averaged atmospheric circulation (Figure 5a) where moisture fluxes across the African, American, and Southeast Asian boundaries are initially replaced by the corresponding integrals of $[\overline{qu}]$, that is, the gray numbers in Figure 4. The implied net $\overline{P-E}$ over each ocean basin is then computed from the modified Q_{AB}, Q_{CD}, and Q_{EF} keeping fluxes across the Arctic and SO boundaries unchanged.

If the fluxes across AB, CD, and EF each matched $[\overline{qu}]$ (Figure 5a), $\overline{P-E}$ would be negative in the Pacific, Atlantic, and Indian Ocean basins as expected (see section 1). Furthermore, the three ocean basins would have similar $\overline{P-E}$ per unit area (Table S3). This also reinforces that moisture fluxes to the Arctic and Antarctic play minor roles in the $\overline{P-E}$ asymmetry. When the flux across Africa is reverted to its "real-world" value, less atmospheric moisture flux leaves the Indian Ocean basin and enters the Atlantic basin, so Indian $\overline{P-E}$ becomes approximately neutral and Atlantic net evaporation is stronger, matching the "real-world" value (Figure 5b). There is very little impact on Pacific and Atlantic $\overline{P-E}$ when the flux across the Americas Q_{EF} is reverted to its "real-world" value since it is almost the same as the integral of $[\overline{qu}]$ (Figure 4a). Reverting the flux across Southeast Asia to its "real-world" value reverses the sign relative to the zonal mean flux (Figure 5c). The Indian Ocean now becomes strongly evaporative, and Pacific $\overline{P-E}$ becomes neutral as seen in Figure 1. In summary, the thought experiment shows that deviations from $[\overline{qu}]$ along the Southeast Asian catchment boundary dominate the $\overline{P-E}$ asymmetry between the Atlantic and Pacific Oceans, as well as between the Indian and Pacific Oceans.

6. Conclusions

Through a process of elimination, it has been deduced that the atmospheric moisture flux across Southeast Asia, especially during the Asian Summer Monsoon, is the dominant factor establishing the $\overline{P-E}$ asymmetry between the Pacific, Atlantic, and Indian Oceans. The steps in the argument eliminating other factors are as follows:

1. Moisture fluxes into the SO basin are dominated by submonthly fluxes which are everywhere poleward with similar Qn' per unit length along each sector of 35°S (Table S2). Therefore, fluxes across the SO boundary do not contribute to the $\overline{P-E}$ asymmetry.
2. Fluxes associated with the monthly mean flow are greater across some segments of the Arctic boundary compared with the poleward flux from the submonthly fluxes. However, the net flux between the Pacific and Arctic is almost zero while there is a net flux into the Arctic from the Atlantic basin of 0.11 Sv. This contributes almost one quarter of the $\overline{P-E}$ asymmetry.
3. Submonthly fluxes (Qn') across the American, African, and Southeast Asian boundaries (Figure S1) are very small compared to the flux by the monthly mean flow.
4. Integral moisture fluxes across the African, Southeast Asian, and American boundaries, Q_{AB}, Q_{CD}, and Q_{EF}, only contribute to ocean basin asymmetry in $\overline{P-E}$ to the extent that they deviate from the zonal mean zonal moisture flux ($[\overline{qu}]$) integrated over the same latitude range. The normal flux across the Americas, Q_{EF}, approximately equals the zonal mean flux and therefore does not contribute to the $\overline{P-E}$ asymmetry (Figures 4 and 5 and Table S3).

The deviation of the flux across Southeast Asia, Q_{CD}, from $[\overline{qu}]$ dominates the annual mean state of the asymmetry. The net eastward moisture flux of 0.59 Sv during the Asian Summer Monsoon generates a large deviation from the westward zonal mean flux even in the annual average. This causes annual mean Pacific $\overline{P-E}$ to be approximately neutral rather than the net evaporation ($\overline{P-E} \approx -0.66$ Sv) calculated using zonal mean fluxes across the latitude range of boundary CD (Figure 4).

The seasonal cycles of Q_n and $\overline{P-E}$ show that Southeast Asian Q_n changes direction, and African Q_n weakens, during the Asian Summer Monsoon in JJA. This results in a strong excess of precipitation over evaporation across the Pacific, a peak in Indian Ocean net evaporation (Figure 3c) and also a reduction of moisture flux into the Atlantic across Africa. The role of the Asian Monsoon has been identified as an important factor previously (Czaja, 2009; Emile-Geay et al., 2003; Ferreira et al., 2018), but we present the first quantification of its impact and argue that it affects the basin scale asymmetry, rather than just the subpolar asymmetry between the Atlantic and Pacific Oceans.

Data Availability Statement

The data set defining the ocean catchment boundaries is available from the University of Reading Research Data Archive (https://doi.org/10.17864/1947.195). The ERA-Interim data set was made available by ECMWF.

Acknowledgments
The lead author received PhD studentship funding from the Natural Environment Research Council as part of the SCENARIO Doctoral Training Partnership (NE/L002566/1).

References

Baker, A. J., Sodemann, H., Baldini, J. U. L., Breitenbach, S. F. M., Johnson, K. R., van Hunen, J., & Pingzhong, Z. (2015). Seasonality of westerly moisture transport in the East Asian summer monsoon and its implications for interpreting precipitation $\delta^{18}O$. *Journal of Geophysical Research: Atmospheres*, *120*, 5850–5862. https://doi.org/10.1002/2014JD022919

Berrisford, P., Kållberg, P., Kobayashi, S., Dee, D., Uppala, S., Simmons, A. J., et al. (2011). Atmospheric conservation properties in ERA-Interim. *Quarterly Journal of the Royal Meteorological Society*, *137*, 1381–1399.

Broecker, W. S. (1991). The Great Ocean Conveyor. *Oceanography*, *4*, 79–89.

Clarke, A. J. (1988). Inertial wind path and sea surface temperature patterns near the Gulf of Tehuantepec and the Gulf of Papagayo. *Journal of Geophysical Research*, *93*, 15,491–15,501.

Craig, P. M. (2018). The Atlantic/Pacific atmospheric moisture budget asymmetry: The role of atmospheric moisture transport (PhD Thesis).

Craig, P. (2019). Catchment boundaries of ocean drainage basins. University of Reading. Dataset: https://doi.org/10.17864/1947.195

Craig, P. M., Ferreira, D., & Methven, J. (2017). The contrast between Atlantic and Pacific surface water fluxes. *Tellus A*, *69*(1330454).

Czaja, A. (2009). Atmospheric control on the thermohaline circulation. *Journal of Climate*, *39*, 234–247.

Dai, A., & Trenberth, K. E. (2002). Estimates of freshwater discharge from continents: Latitudinal and seasonal variations. *Journal of Hydrometeorology*, *3*, 660–687.

Dee, D. P., Uppala, S. M., Simmons, A. J., Berrisford, P., Poli, P., Kobayashi, S., et al. (2011). The ERA-Interim reanalysis: Configuration and performance of the data assimilation system. *Quarterly Journal of the Royal Meteorological Society*, *137*, 553–597.

Dey, D., & Döös, K. (2019). The coupled ocean–atmosphere hydrologic cycle. *Tellus A*, *71*, 1,650,413.

Emile-Geay, J., Cane, M. A., Naik, N., Seager, R., Clement, A. C., & van Geen, A. (2003). Warren revisited: Atmospheric freshwater fluxes and "Why is no deep water formed in the North Pacific". *Journal of Geophysical Research*, *108*(6), 3178. https://doi.org/10.1029/2001JC001058

Ferreira, D., Cessi, P., Coxall, H., de Boer, A., Dijkstra, H. A., Drijfhout, S. S., et al. (2018). Atlantic-Pacific asymmetry in deep water formation. *Annual Reviews of Earth and Planetary Sciences*, *46*(1), 327–352.

Ferreira, D., Marshall, J., & Campin, J.-M. (2010). Localization of deep water formation: Role of atmospheric moisture transport and geometrical constraints on ocean circulation. *Journal of Climate*, *23*, 1456–1476.

Goswami, B. N., & Sengupta, D. (2003). A note on the deficiency of NCEP/NCAR reanalysis surface winds over the equatorial Indian Ocean. *Journal of Geophysical Research*, *108*, 3124. https://doi.org/10.1029/2002JC001497

Leduc, G., Vidal, L., Tachikawa, K., Rostek, F., Sonzogni, C., Beaufort, L., & Bard, E. (2007). Moisture transport across Central America as a positive feedback on abrupt climatic changes. *Nature*, *445*, 908–911.

Levang, S. L., & Schmitt, R. W. (2015). Centennial changes of the global water cycle in CMIP5 models. *Journal of Climate*, *28*, 6489–6502.

Lohmann, G. (2003). Atmospheric and oceanic freshwater transport during weak Atlantic overturning circulation. *Tellus A*, *55*, 438–449.

Manabe, S., & Stouffer, R. J. (1988). Two stable equilibria of a coupled ocean-atmosphere model. *Journal of Climate*, *1*, 841–866.

Nicholson, S. (2016). The Turkana low-level jet: Mean climatology and association with regional aridity. *International Journal of Climatology*, *36*, 2598–2614.

Pfahl, S., O'Gorman, P., & Singh, M. S. (2015). Extratropical cyclones in idealized simulations of changed climates. *Journal of Climate*, *28*, 9373–9392.

Richter, I., & Xie, S.-S. (2010). Moisture transport from the Atlantic to the Pacific basin and its response to North Atlantic cooling and global warming. *Climate Dynamics*, *35*, 551–566.

Riddle, E. E., & Cook, K. H. (2008). Abrupt rainfall transitions over the Greater Horn of Africa: Observations and regional model simulations. *Journal of Geophysical Research*, *113*, D15109. https://doi.org/10.1029/2007JD009202

Rodriguez, J. M., Johns, T. C., Thorpe, R. B., & Wiltshire, A. (2011). Using moisture conservation to evaluate oceanic surface freshwater fluxes in climate models. *Climate Dynamics*, *37*, 205–219.

Schiemann, R., Demory, M.-E., Mizielinski, M. S., Roberts, M. J., Shaffrey, L. C., Strachan, L. C., & Vidale, P. L. (2014). The sensitivity of the tropical circulation and Maritime Continent precipitation to climate model resolution. *Climate Dynamics*, *42*, 2455–2468.

Schmitt, R. W., Bogden, P. S., & Dorman, C. E. (1989). Evaporation minus precipitation and density fluxes for the North Atlantic. *Journal of Physical Oceanography*, *19*, 1208–1221.

Schmittner, A., Silva, T. A. M., Fraedrich, K., Kirk, E., & Lunkeit, E. (2011). Effects of mountains and ice sheets on global ocean circulation. *Journal of Climate*, *24*, 2814–2829.

Singh, H. K. A., Donohoe, A., Bitz, C. M., Nusbaumer, J., & Noone, D. C. (2016). Greater moisture transport distances with warming amplify interbasin salinity contrasts. *Geophysical Research Letters*, *43*, 8677–8684. https://doi.org/10.1002/2016GL069796

Sinha, B., Blaker, A. T., Hirschi, J.-M., Bonham, S., Brand, M., Josey, S., et al. (2012). Mountain ranges favour vigorous Atlantic meridional overturning. *Geophysical Research Letters*, *39*, L02705. https://doi.org/10.1029/2011GL050485

Steenburgh, W. J., Schultz, D. M., & Colle, B. A. (1998). The structure and evolution of gap outflow over the Gulf of Tehuantepec, Mexico. *Monthly Weather Review*, *126*, 2673–2691.

Stohl, A., & James, P. (2005). A Lagrangian analysis of the atmospheric branch of the global water cycle. Part II: Moisture transports between Earth's ocean basins and river catchments. *Journal of Hydrometeorology*, *6*, 961–984.

Trenberth, K. E., & Caron, J. M. (2001). Estimates of meridional atmosphere and ocean heat transports. *Journal of Climate*, *14*, 3433–3443.

Trenberth, K. E., Fasullo, J. T., & Mackaro, J. (2011). Atmospheric moisture transports from ocean to land and global energy flows in reanalyses. *Journal of Climate*, *24*, 4907–4924.

Volonté, A., Turner, A. G., & Menon, A. (2019). Airmass analysis of the processes driving the progression of the Indian summer monsoon. *Quarterly Journal of the Royal Meteorological Society*, *146*, 2949–2980.

Wang, C., Zhang, L., & Lee, S.-K. (2013). Response of freshwater flux and sea surface salinity to variability of the Atlantic warm pool. *Journal of Climate*, *26*, 1249–1267.

Warren, B. A. (1983). Why is no deep water formed in the North Pacific? *Journal of Marine Research*, *41*, 327–347.

Wills, R. C., & Schneider, T. (2015). Stationary eddies and the zonal asymmetry of net precipitation and ocean freshwater forcing. *Journal of Climate*, *28*, 5115–5133.

Zaucker, F., & Broecker, W. S. (1992). The influence of atmospheric moisture transport on the fresh water balance of the Atlantic drainage basin: General circulation model simulations and observations. *Journal of Geophysical Research*, *97*, 2765–2773.